

Blue copper proteins as a model for investigating electron transfer processes within polypeptide matrices

O. Farver ^a, I. Pecht ^{*,b}

^a *Institute of General Chemistry, Royal Danish School of Pharmacy, Copenhagen 2100, Denmark*

^b *Department of Chemical Immunology, The Weizmann Institute of Science, Rehovot 76100, Israel*

(Received 5 January 1994)

Abstract

Intramolecular long-range electron transfer (ET) processes have been investigated in two types of blue copper proteins; the single-copper protein, azurin and the multi-copper oxidase, ascorbate oxidase. These have several advantages for investigating the parameters that control the above reactions: (1) Their sole physiological role is mediating or catalyzing ET processes via the evolutionary optimized copper sites. (2) The three-dimensional structures of a considerable number of blue single copper containing proteins, e.g. azurins, and of ascorbate oxidase, have been determined at high resolution. (3) These proteins have no other cofactors except for the copper ions, thus the role of the polypeptide matrix can be addressed in a more straightforward manner. In azurins, the ET from the cystine (3–26) radical-ion produced by pulse-radiolytic reduction of this single disulfide bridge, to the Cu(II) ion bound at a distance of ≈ 2.6 nm has been studied, in naturally occurring and in single-site mutated azurins. The role of changing specific amino acid residues on the internal long-range electron transfer (LRET) process and its potential pathways has been investigated. It is noteworthy that this process is most probably not part of the physiological function of azurin, hence, there has not been any evolutionary selection of structural elements for the reaction. Therefore, this provides a system for an unbiased examination of structural and chemical requirements for control of this process. By contrast, in blue copper oxidases, the internal ET from the electron uptake site from substrate to the O₂ reduction site is part of these enzymes catalytic cycle, presumably optimized by selective pressure. We are investigating this internal ET in ascorbate oxidase and try to resolve the relation between this enzyme's distinct functional states and the internal ET rates. We conclude that in both types of proteins, the investigated LRET proceed primarily along covalent pathways, thus providing suitable systems where the parameters controlling the efficiency of these processes can be pursued.

Key words: Ascorbate oxidase; Azurin; Pathway calculation; Pulse radiolysis

1. Introduction

Electron transfer (ET) is one of the simplest of all chemical reactions [1]. Still, since life on earth

* Corresponding author. Fax 972-8-4652 64.

derives its energy via photosynthesis and respiration, our very existence depends on this fundamental process. Biological ET processes usually take place between and within proteins where the redox centers are bound and separated sometimes by considerable distances ($> 10 \text{ \AA}$) [2]. Attention of both theoreticians and experimentalists has been devoted to studying these processes. The present understanding of protein-mediated ET has advanced, in particular due to the following: site directed mutagenesis has provided a most effective tool for introducing highly selective changes in the amino acid sequence of proteins and studying the effects on ET processes. This was accompanied by the determination of three-dimensional structures of an increasing number of redox proteins. Finally, the theoretical models for long-range electron transfer (LRET) have now reached a form which can be more readily used by experimentalists [1–4].

Here we wish to briefly review results of our studies of intramolecular long-range electron transfer in two different types of “blue” copper proteins: the single-copper protein, azurin, and the copper enzyme, ascorbate oxidase which contains four copper ions per active subunit. It is further our intention to illustrate how the experimental results can be rationalized in the framework of the current theoretical treatments of LRET.

The blue copper proteins have several advantageous features for serving as model systems for investigating ET within the polypeptide matrix [5]; first and foremost all these proteins’ function is electron transfer and the blue copper site has apparently evolved so as to undergo minimal structural rearrangements upon the Cu(II/I) redox cycle [6]. Second, the copper ions are directly coordinated to amino acid residues with no other intervening prosthetic groups. Thus, the medium separating the redox partners is only the protein matrix itself.

2. The nature of ET within proteins

Electron transfer in proteins shares common features with that of small molecules yet has also

its distinct properties [1]. In both cases the active centers are expected to undergo changes in their intrinsic structure as well as in their solvation and other forms of medium reorganization. Therefore, the ET rates are expected to depend on the energy required for bond-length and angle changes and solvent reorientation accompanying the ET. In proteins the ET process involves, however, the surrounding polypeptide matrix as the medium. This is far less homogeneous than the solvent molecules surrounding the partners in a small molecule ET reaction. Moreover, protein conformational transitions may precede or follow ET and may affect the free energy change of the reactions. Further, most ET reactions between small molecules in solution are expected to take place between reactants in close contact whereas in proteins the redox centers are in fixed positions within the polypeptide matrix and hence prevented from coming in direct contact. Therefore, the ET rate is expected to depend on the distance between electron donor and acceptor. Finally, there is the intriguing question of whether the nature of the intervening medium between electron donor and acceptor affects the reaction rate or more specifically; did evolutionary pressure select protein structure elements that promote or suppress ET rates through them. Thus, it has frequently been suggested [5,7,8] that delocalized low-lying π^* orbitals of aromatic systems make such residues play an important role in promoting electron transfer, and indeed some evidence has been documented experimentally [7–9]. However, an advantageous π electron conduction is expected only in cases where such side chains are closely packed and favourably oriented.

The above aspects are being studied by us in the two prototype blue copper proteins, azurin (Az) and ascorbate oxidase (AO) and the progress made so far will be presented in this short review.

3. Theory

The theory of ET has been reviewed in several excellent articles [1–4,10,11]. Here we only wish

to present a short summary of the relevant concepts and equations which will be used in the following review. In protein long-range ET, where weak coupling operates between the electron donor and acceptor sites, the rate will be proportional to the square of the protein mediated electronic coupling between the reactant and product electronic states which are described in the form of a matrix element, H_{AB} . For an intramolecular ET, the rate constant is given by Fermi's Golden Rule;

$$k = \frac{2\pi}{\hbar} H_{AB}^2 (\text{FC}). \quad (1)$$

The quantity (FC) is the Franck–Condon nuclear factor which, for relatively low vibrational frequencies, in the high-temperature region, (i.e. if $kT > h\nu$) can be treated classically. This situation often applies to biological ET around room temperature, and the nuclear rearrangements of the solvent and within the protein itself can thus be expressed in a simple form (Eq. (2)). The electronic motion, however, requires a quantum mechanical treatment. The semi-classical Marcus expression thus takes the form [1]

$$k = \frac{2\pi}{\hbar} \frac{H_{AB}^2}{(4\pi\lambda RT)^{1/2}} e^{-(\Delta G^0 + \lambda)^2 / 4\lambda RT}. \quad (2)$$

This equation shows that the ET rate increases with temperature when the driving force ($-\Delta G^0$) is less than the reorganization energy, λ , reaches a maximum when $-\Delta G^0 = \lambda$ and then actually decreases again. Just as simple wave functions decay exponentially with distance, it is also expected that the tunneling matrix element, H_{AB}^2 will fall off exponentially with the distance $r - r_0$

$$H_{AB} = H_{AB}^0 e^{-\frac{1}{2}\beta(r-r_0)} \quad (3)$$

and so will the ET rate constant. H_{AB}^0 is the electronic coupling at close contact ($r = r_0$). The decay of electronic coupling with distance is given by the coefficient β which describes the overall effect of the medium separating electron donor and acceptor. One of the more challenging questions is now whether only the distance plays a role or the medium as well. Are specific pathways

employed and can the polypeptide matrix modulate ET rates? Estimates of the exponential decay factor, β have been made by theoreticians which, in turn, have stimulated experimentalists to try and verify the predictions [1–4].

When LRET is treated as an electron tunneling from donor to acceptor via the protein acting as a bridge comprised of distinct elements (e.g. chemical bonds), H_{AB} would simply decrease by a multiplicative coupling factor, ϵ , as the chain extends [12]. In proteins, the covalent path connecting donor with acceptor can be very long compared to the direct “through-space” distance. In calculating such pathways, the protein structure is analyzed for combinations of bonding and non-bonding links which maximize H_{AB} . The resultant pathway will mostly be constituted of covalent and hydrogen bonds and possibly some through-space jumps (van der Waals contacts). Semi-empirical expressions for the ϵ factors have been derived [12,13],

$$\begin{aligned} \epsilon_C &= 0.6, \\ \epsilon_H &= \epsilon_C^2 \exp[-1.7(r - 2.8)], \\ \epsilon_S &= \frac{1}{2}\epsilon_C \exp[-1.7(r - 1.4)], \end{aligned} \quad (4)$$

for covalent (C), hydrogen bonded (H) and through-space interactions (S). The tunneling matrix element, H_{AB} can then be written as

$$H_{AB} = P \prod_i \epsilon_{C(i)} \prod_j \epsilon_{H(j)} \prod_k \epsilon_{S(k)}, \quad (5)$$

where the prefactor, P depends on the interaction of donor and acceptor with the bridging orbitals.

4. Pulse radiolysis

Pulse radiolysis enables the production, within a fraction of a microsecond, of either reducing or oxidizing chemical entities in an aqueous solution [14]. This is attained by introducing short pulses of high-energy electrons (e.g. 5 MeV) produced by a linear accelerator. Interaction of these accelerated electrons occurs practically with solvent water molecules only and the detailed chemistry

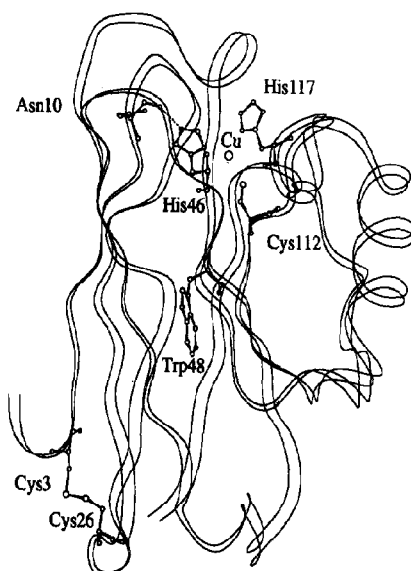
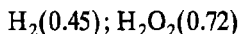
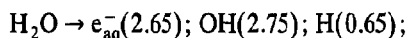


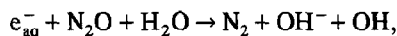
Fig. 1. Three-dimensional structure of the polypeptide backbone of *Pseudomonas aeruginosa* azurin [19]. Some amino-acid residues of particular interest have been included.

of the ensuing processes has been worked out in detail [15]. Thus, the following species are produced with yields per 100 eV of absorbed energy given in parentheses,

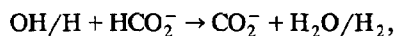


Particularly prominent for their reactivity are the first two, with potentials at both extremes of the aqueous solutions redox scale (E^0 of $\text{e}_{\text{aq}}^- \approx -2.7$ V and E^0 of $\text{OH} \approx 1.8$ V). By a series of

well designed reactions, these initial products can be converted into milder reductants or oxidants. This can be illustrated by the protocol employed for production of the CO_2^- radical ($E^0 = -1.05$ V). In neutral, N_2O saturated solutions containing sodium formate (0.1 M), the following sequence takes place:



$$k = 8.7 \times 10^9 \text{ M}^{-1} \text{ s}^{-1},$$



$$k_{\text{OH}} = 3 \times 10^9 \text{ M}^{-1} \text{ s}^{-1},$$

$$k_{\text{H}} = 3 \times 10^8 \text{ M}^{-1} \text{ s}^{-1}.$$

Thus, within microseconds, a concentration of up to several micromolar CO_2^- can be produced in an aqueous solution of a given protein. With an appropriate fast optical detection system, reliable measurements of ET reactions can be carried out in a time range from less than 1 μs into the minutes domain.

5. LRET in azurin

Azurins belong to the family of blue single copper proteins [16,17]. It is assumed to function as an electron mediator in the energy conversion system of several bacteria. While different azurins were found to be rather similar in their three-dimensional structure [6,18–20] (Fig. 1), marked differences do exist in their amino acid sequences, hence providing proteins with distinct

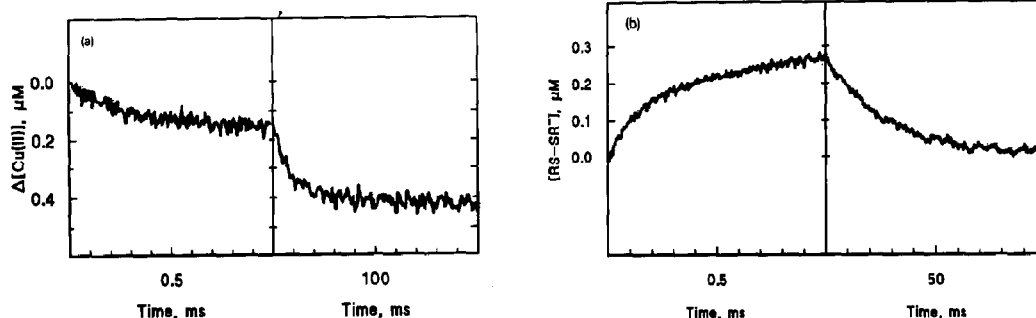


Fig. 2. Time resolved absorption changes observed at 625 nm (a) and 410 nm (b) in the single-site mutated (H35Q) azurin upon reduction by CO_2^- radicals. The conditions were: Temperature 286 K; pH 7.0; pulse width 0.5 μs .

reactivities and reduction potentials. All known azurins contain a disulfide bridge at one end of its β -sandwich structure, at a distance of 2.6 nm from the copper binding site present at the opposite end of the protein. High-resolution three-dimensional structures are now available for a number of both wild-type and single-site mutated azurins [6,18–20] providing an interesting system for examining the effect of the different parameters which control the rate of LRET.

When oxidized azurin reacts with CO_2^- , the latter radicals were found to react, at practically diffusion controlled rates, with both the Cu(II) ion and the disulfide bridge [21–24]. These processes can be clearly monitored via the optical absorption bands of Cu(II) and RSSR $^-$ as illustrated in Fig. 2. When the main absorption band of the protein bound Cu(II) is monitored ($\epsilon_{625} = 5700 \text{ M}^{-1} \text{ cm}^{-1}$), the fast reduction phase was found to be a second-order process corresponding to a direct bimolecular reduction of the Cu(II) center by CO_2^- radicals. A rapid increase in absorption was observed when the reaction was followed at 410 nm, due to the formation of the disulfide RSSR $^-$ radical which has a strong absorption band centered at that wavelength ($\epsilon_{410} \approx 10000 \text{ M}^{-1} \text{ cm}^{-1}$). When absorption changes were monitored at slower time domains, the 410 nm band was found to disappear concomitantly with a further decrease in absorption at 625 nm (Fig. 2). The specific rates of these two slower processes were found to be identical. Also, the respective amplitudes were the same. Taken together these results strongly suggested that the observed processes are due to an electron being transferred intramolecularly from the disulfide radical anion to the Cu(II) site. The rate constants of both processes were independent of the reductant ($0.5\text{--}6.5 \mu\text{M}$) and protein concentrations ($2\text{--}10 \mu\text{M}$) demonstrating that both are unimolecular, as expected for an intramolecular process. The specific rates determined at pH 7 and 298 K are summarized, together with the respective Cu(II)/Cu(I) reduction potentials, in Table 1 for azurins isolated from different bacteria and for single-site mutated *Ps. aeruginosa* azurins.

The data of Table 1 are also presented in

Table 1

Kinetic and thermodynamic data for the intramolecular reduction of Cu(II) by RSSR $^-$

Azurin	k_{298} (s $^{-1}$)	E' (mV)	$-\Delta G^\circ$ (kJ mol $^{-1}$)	ΔH° (kJ mol $^{-1}$)	ΔS° (J K $^{-1}$ mol $^{-1}$)
Wild type					
<i>Ps. aer</i> ^a	44 \pm 7	304	68.9	47.5 \pm 4.0	-56.5 \pm 7.0
<i>Ps. fluor.</i> ^b	22 \pm 3	347	73.0	36.3 \pm 1.2	-97.7 \pm 5.0
<i>Alc. spp.</i> ^a	28 \pm 2	260	64.6	16.7 \pm 1.5	-171 \pm 18
<i>Alc. faec.</i> ^b	11 \pm 2	266	65.2	54.5 \pm 1.4	-43.9 \pm 9.5
Mutant					
W48L ^c	40 \pm 4	323	70.7	48.3 \pm 0.9	-51.5 \pm 5.7
W48M ^c	33 \pm 5	312	69.7	48.4 \pm 1.3	-50.9 \pm 7.4
F114A ^c	72 \pm 14	358	74.1	52.1 \pm 1.3	-36.1 \pm 8.2
M121L ^c	38 \pm 7	412	79.3	45.2 \pm 1.3	-61.5 \pm 7.2
M44K ^d	134 \pm 12	370	75.3	47.2 \pm 0.7	-46.4 \pm 4.4
H35Q ^d	53 \pm 11	268	65.4	37.3 \pm 1.3	-86.5 \pm 5.8

^a Ref. [21]. ^b Ref. [22]. ^c Ref. [23]. ^d Ref. [24].

another way in Fig. 3, where the observed rate constants for intramolecular ET in azurin are plotted against the Cu(II)/Cu(I) reduction potentials. Assuming that the disulfide/radical potential is not altered in the different azurins, Fig. 3 represents the dependence of the rate on the

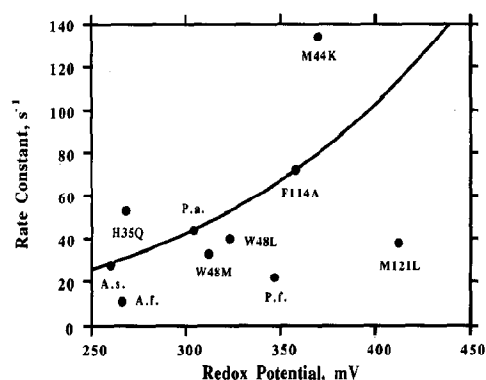


Fig. 3. Observed rate constants for the intramolecular RSSR $^-$ to Cu(II) ET in different azurins at 298 K, plotted against the measured reduction potentials of the Cu(II)/Cu(I) pair. Assuming a constant potential of -410 mV for the disulfide/radical the X axis represents the driving force of the ET reaction. The individual azurins are identified on the figure. WT: P.a. *Pseudomonas aeruginosa*; P.f. *Pseudomonas fluorescens* biotype B; A.f. *Alcaligenes faecalis*; A.s. *Alcaligenes* species. The mutants labeling refers to those made in the P.a. sequence.

driving force of the reaction. Using WT *Ps. aeruginosa* azurin as a reference and a reorganization energy of $\lambda = 134 \text{ kJ mol}^{-1}$ (*vide infra*) the expected rate constants were calculated assuming that the driving force was the only parameter responsible for changes in the ET rates of the different azurins. While there seems to be some correspondence, there are also several conspicuous deviations which will be discussed below. The temperature dependence of the LRET rates was examined over a temperature range from 4.2 to 42.7°C at pH 7.0 and the derived activation parameters are also summarized in Table 1.

6. Electron transfer pathways calculations

Pathway calculations employed the high-resolution three-dimensional structures of *Ps. aeruginosa* azurin and its mutants when available [19,20].

Alternatively, structures were calculated for the single-site mutated azurins. Spectroscopic studies, mainly performed by NMR and ESR, have strongly suggested that single-site mutations outside the copper coordination shell have little effect on the structure of the metal site [25]. This is supported by comparison of the high-resolution structures of the WT *Ps. aeruginosa* azurin (210 pm) and its H35Q mutant (190 pm) which show the two proteins to be practically identical with the exception of the structure at and immediately next to the mutated residue [19].

The pathway calculations predict similar electron transfer rates in the native and the mutated proteins studied so far. Two main pathways were found with small differences in the electronic coupling factors, between the wild-type and the mutated azurins (Table 2 and Fig. 4): one distinct pathway proceeds through the polypeptide backbone from Cys3 to Asn10 followed by the hydro-

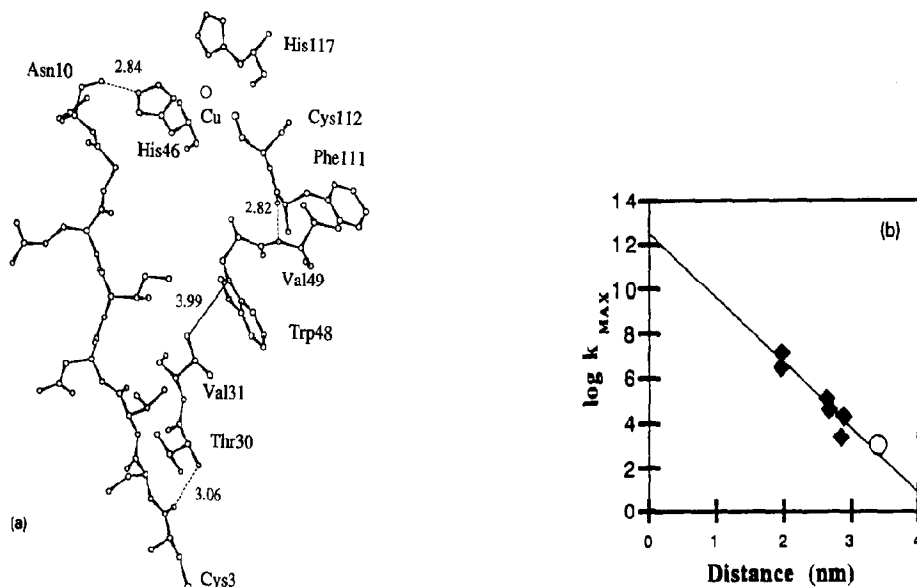


Fig. 4. (a) Calculated ET pathways from the disulfide to the copper centre in *Ps. aeruginosa* azurin. Some of the interconnecting distances (in Å) are shown. Hydrogen bonds are indicated by a broken line, and the through-space jump by an extended line. In the two mutants where Trp 48 is substituted by Met or Leu, the distances from Val 31-C γ to Met48-C γ and Leu48-C γ are 3.81 and 3.72 Å, respectively. The coordinates were taken from ref. [19]. (b) Plot of $\log k_{\text{MAX}}$ versus the through-bond distance for Ru-modified cytochromes (■) [13] and for WT azurin (○) [21]. The straight line is drawn with a slope of $\beta = 6.7 \text{ nm}^{-1}$.

Table 2

Electronic decay factors, π_{ei} , for the two main ET pathways from the disulfide radical to Cu(II) in azurin, cf. Fig. 4

Azurin	$10^8 \pi_{ei}$	
	through backbone	via residue 48
WT	24.6	2.6
W48L	24.6	4.0
W48M	24.6	3.4
F114A	31.2	3.0
M121L	31.4	2.7
M44K	34.9	3.1
H35Q	17.5	0.7

gen bond between its carboxyl to the N(ϵ)H of the imidazole copper ligand (His46). The second pathway goes directly from Cys3 to Thr30 via a hydrogen bond, and then from Val31 via a through-space jump of about 0.4 nm to Trp48 (or, in the mutants, Met48 and Leu48, respectively), then to Val49 and from it to Phe111 by another hydrogen bond, continuing by polypeptide backbone connection to the thiolate copper ligand of Cys112 (Fig. 4a).

7. LRET in azurin as a model

The temperature dependence of the intramolecular ET rate constants (Table 1) can be analyzed in terms of the semi-classical Marcus treatment of electron exchange between spatially fixed and oriented redox sites [1] using eqs. (6)–(8),

$$k = \kappa(r) \nu e^{-\Delta G^*/RT} \quad (6)$$

where the activation free energy is:

$$\Delta G^* = \Delta H^* - T\Delta S^* = \frac{\lambda}{4} \left(1 + \frac{\Delta G^0}{\lambda} \right)^2 \quad (7)$$

Here κ is the electronic transmission coefficient, ν is a nuclear vibration frequency and λ is the total reorganization energy. Eqs. (6) and (7) are just another way of expressing Eq. (2), given above.

For nonadiabatic processes the electronic transmission coefficient is, in accordance with Eq. (3) given by

$$\kappa(r) \nu = 10^{13} e^{-\beta(r-r_0)} \quad (8)$$

Here β is the electronic decay factor, and r_0 is the distance at which $\kappa(r) \nu$ equals some preassigned value, $k_B T/h \sim 10^{13} \text{ s}^{-1}$ at 298 K.

Since our pathway calculations suggest that the same route is used for LRET from RSSR⁻ to Cu(II) in all azurins studied so far (Table 2 and Fig. 4), we used the following approach in order to independently derive both the reorganization energy and the electronic decay factor. The substitution of Phe by Ala in the F114A mutant is a relatively innocent one, so we may assume that both β and λ would be the same for the WT protein and this mutant. Combining thermodynamic data (Table 1) for WT *Ps. aeruginosa* and F114A azurins we calculate $\lambda = 134 \text{ kJ mol}^{-1}$ and $\beta(r-r_0) = -22.6$. This is in reasonably good agreement with the value calculated earlier for WT azurin [22]. With a through-bond distance (including the 0.28 nm H bond between Asn10 and His46) of 3.7 nm (i.e. $(r-r_0) = 3.4 \text{ nm}$) this gives $\beta = -6.7 \text{ nm}^{-1}$, which is in excellent agreement with the experimentally determined decay factor for electron tunneling in ruthenated cytochromes (6.8 nm^{-1}) [26] (cf. Fig. 4b) and the one calculated for tunneling through a saturated-(CH₂)_n-chain (6.5 nm^{-1}) [27]. With this value of β we may now calculate the reorganization energy in the M121L mutant, and find it to be 13 kJ larger than for the other mutants we have studied so far. In this mutant the copper ligating Met121 is substituted by a non-ligating leucine residue, and the reorganization energy may be altered so as to counteract the increase in rate expected on the basis of the larger driving force (cf. Table 1). Fig. 3 demonstrates that in M44K the rate is almost twice as fast as expected from the Cu(II)/Cu(I) reduction potential. Here a methionine residue in a hydrophobic area, close to the copper center has been exchanged by lysine which certainly affects the solvent reorganization energy near the copper centre. Indeed, a decrease in the reorganization energy from $\lambda = 134 \text{ kJ mol}^{-1}$ for

native azurin to 129 kJ mol^{-1} would account for the discrepancy. The four points in Fig. 3 representing azurins which have Trp48 substituted by non-aromatic residues, lie below the calculated line. There is no *a priori* reason for these proteins to have reorganization energies different from that of the WT *Ps. aeruginosa* azurin. Hence the slower rates might be due to changes in the distance between electron donor and acceptor or to the specific nature of the aromatic residue. However, the model calculations show that the distances through the residue-48 pathway become shorter, giving a slightly better electronic coupling in the pathway calculations (cf. Table 2 and Fig. 4). The discrepancy between the pathway calculations and observed rate constants for the four azurin species lacking Trp48 could then be due to the pathway calculations not taking into account the aromatic nature of the indole side chain.

The difference between experimentally determined and calculated LRET rates resolved by this comparison is quite small, (cf. Fig. 3) in line with the calculations (Table 2) as the route including the indole of Trp48 has an electronic coupling factor about ten times smaller than that of the longer pathway via the backbone. This suggests that the pathway involving residue 48 only plays a minor role in this LRET in the azurins studied so far. It is also noteworthy that the above calculations do not distinguish between pathways involving σ - and π -orbital systems. In an earlier theoretical analysis, Broo and Larsson [27] applied an extended Hückel method to the LRET reaction in WT *Ps. aeruginosa* azurin assuming the operation of the above two pathways. In contrast to the present results, they found that the route involving Trp48 is ten times more efficient than through the backbone. However, their conclusions were somewhat indecisive in that removal of the Trp48 indole ring would reduce the rate five fold, while removal of two additional aromatic rings (Phe15 and Phe29) restored the calculated rate constant value to that of the wild-type protein. In addition, only unrefined 3D coordinates were available at the time these calculations were made and the removal of the aromatic residues was performed with no readjustment of

the structure. Hence, further calculations with this method are required before a better comparison between the two computational procedures can be made.

The role of the protein matrix in LRET is still a matter of active discussion [28–31]. While there is substantial evidence for through-bond ET, Moser et al. have recently analyzed data obtained from studies of a large variety of intramolecular electron transfer reactions and found that the free energy optimized rate constants for many “biological” ET processes correlate well with the edge-to-edge distance between donor and acceptor, with a decay factor, $\beta = 14 \text{ nm}^{-1}$ [28–29]. The distance $r - r_0$ between S γ of Cys26 and S γ of Cys112, which represents the shortest edge-to-edge distance between electron donor and acceptor derived from the refined *Ps. aeruginosa* azurin structure, is 2.46 nm [20]. This yields $\beta = 9 \text{ nm}^{-1}$. The difference in the above β values is too large to be accounted for in terms of experimental error. Further, the calculated maximum LRET rate constant for azurin (i.e. for $\lambda = -\Delta G^0$) is 10^3 s^{-1} while using the correlation line of Moser et al. the rate constant should be two orders of magnitude smaller. We may therefore conclude that our data do not fit an exponential-decay correlation with direct through-space distance. Rather, $k_{\text{MAX}} = 10^3 \text{ s}^{-1}$ fits perfectly on a linear plot of $\log k_{\text{MAX}}$ versus the through-bond distance for Ru-substituted cytochrome-c drawn with a slope of 6.7 nm^{-1} (Fig. 4b).

In discussing the LRET between RSSR $^-$ and Cu(II) in azurins, one should also keep in mind that this protein's physiological function is confined to the redox cycle of the copper site and the above internal process is most likely a *non*-physiological one. Hence no pathway is a product of evolutionary optimization. In fact, the disulfide is situated in a “cold” spot (area with a relatively low electronic coupling with the Cu(II) ion) on the azurin molecule as nicely illustrated by Beratan et al. [12]. In systems that were evolutionarily selected for efficient electron transfer, aromatic residues may be found positioned so as to considerably enhance the electronic coupling. Examples of this are the tryptophan-mediated reduction of quinone in the photosynthetic reaction

center [7], the tryptophan function in the CCP:CC complex [9] and Tyr83 in plastocyanin [8].

8. Intramolecular LRET in ascorbate oxidase is part of the catalytic cycle

The blue copper oxidases are redox enzymes that catalyze specific, one-electron substrate oxidation by dioxygen, which in turn is reduced to two water molecules [5,32]. Their minimal catalytic unit contains four copper ions bound to distinct sites classified according to the unique spectroscopic properties conferred on the bound copper ions. The Type 1 (T1) site is rather similar to the copper coordination site found in the single blue copper proteins. A pair of Cu(II) ions is bound to a site designated as the Type 3 (T3) characterized by an absorbance band in the near-UV region and by its being anti-ferromagnetically coupled. Together with the proximal Type 2 (T2) Cu(II) site [33,34], which has a rather weak opti-

cal absorption spectrum and exhibits a typical Cu(II) hyperfine EPR signal, these three ions constitute a trinuclear copper center.

Ascorbate oxidase (AO) is the first member of this family of enzymes for which a high-resolution 3D structure was determined [34,35]. It is a 140 kD protein containing eight copper ions per molecule which were classified into the above T1, T2 and T3 by their spectroscopic properties. The reduction potentials of T1 and T3 are identical at 298 K ($E^0 = 350$ mV, pH 7.0) [36]. The high-resolution three-dimensional model of AO provided unique insights into the detailed structure and spatial relationship among the copper binding sites. Thus, AO has been shown to exist as a dimer of identical 70 kDa subunits, each containing one T1, one T2 and one T3 site. These subunits are folded into three interacting domains, all of similar β -sandwich-type structure, distantly related to the small, blue single copper proteins [34,35]. The Type 1 site, highly conserved among all blue copper proteins, is within one domain. The Type 2 and 3 sites were found

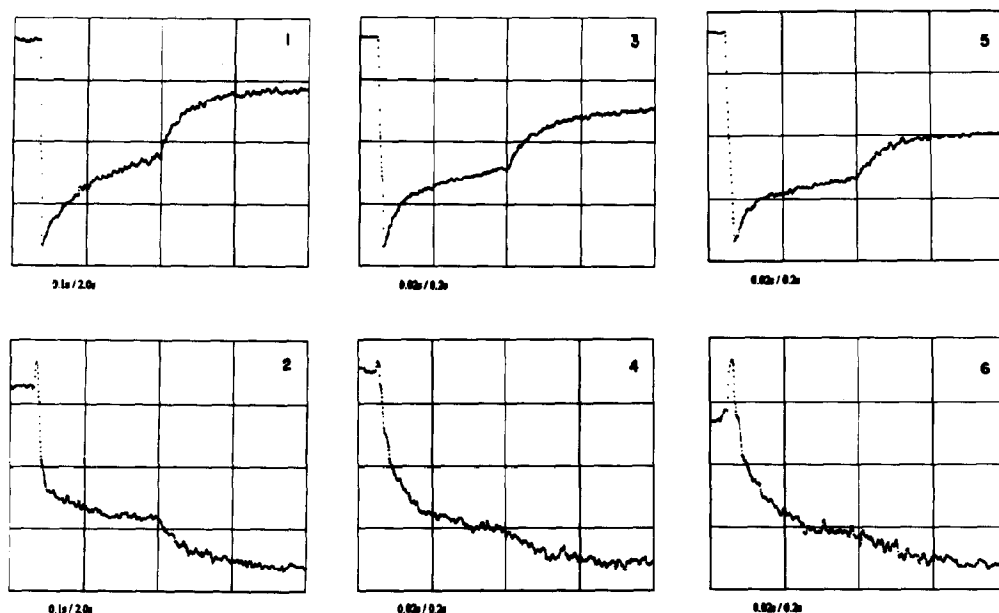


Fig. 5. Time resolved absorption changes monitored at 610 nm (1,3 and 5) and 330 nm (2,4 and 6) in oxidized ascorbate oxidase exposed to a pulse of CO_2^- radicals at pH 5.5 and 285 K; pulse width = 0.7 μs . The absorption changes per division are 0.02 at 610 nm and 0.01 at 330 nm.

to be proximal, thus creating a trinuclear center at a distance of 1.23 nm between the T3 copper pair and the T1 site. Ligands coordinated to the Type 2 and 3 copper ions are provided by the two different domains forming the trinuclear site at the inter-domain region. As stated above, the catalytic cycle of AO is proposed to proceed by a sequential mechanism, where single electrons are provided by the respective substrates (e.g. ascorbate) to the T1[Cu(II)] [36]. The trinuclear (T2/T3) center has been proposed to be the dioxygen reduction site [32]. Thus, intramolecular electron transfer from T1 to T3 has long been assumed to be an essential step required in order to provide the four electrons necessary to yield the final dioxygen reduction product: two water molecules. An intramolecular electron transfer from Type 1 Cu(I) to the oxidized Type 3 site in both laccase [37] and AO [38–40] have recently been observed. Earlier pulse radiolysis studies of the blue oxidases have mainly focused on the kinetics of T1[Cu(II)] reduction and contributed to the notion that the T1 site is the electron uptake site of the blue oxidases [5,36].

When micromolar concentrations of the reducing, pulse radiolytically produced, CO_2^- radical react with oxidized AO under anaerobic conditions, a sequence of ET processes is observed [39]: monitoring optical absorption changes at 610 nm due to the T1 [Cu(II)], the fastest resolvable step was a bimolecular process of direct electron transfer from CO_2^- radicals to T1[Cu(II)], proceeding with a second-order rate constant of $(1.2 \pm 0.2) \times 10^9 \text{ M}^{-1} \text{ s}^{-1}$ (298 K, pH 7.0). Following this step and depending on the extent of AO reduction, either two or three reoxidation steps of this site are observed (the fastest and slowest being of approximately equal intensities) (Fig. 5). From the amplitudes of these absorption changes it is seen that the T1[Cu(I)] is only partly reoxidized. The extent of reoxidation was found to depend on the redox state of the AO molecules at the examined pulse, decreasing from $\approx 90\%$ at oxidized T1 [Cu(II)] sites to $< 10\%$ when the T1 site is close to being fully reduced.

The reactivity of the T3 site with CO_2^- radicals was monitored by following the absorbance changes at 330 nm [39]. While no direct reduction

of the T3[Cu(II)] site by the radicals could be resolved at pH 5.5, at pH 7.0 a considerable amplitude of direct reduction of T3[Cu(II)] was observed though, at a lower second-order rate constant $(6.5 \pm 1.2) \times 10^8 \text{ M}^{-1} \text{ s}^{-1}$. The amplitudes amounted to less than half of the eventual T3 [Cu(II)] reduction in the given pulse. In the slower time domain, reduction of the 330 nm absorption band was observed again proceeding in two or three phases. These reduction steps took place concomitantly with those observed at 610 nm for the reoxidation of T1[Cu(I)], which suggested that both represent the same internal ET processes. Indeed, the respective rate constants of these steps were found, within experimental error, to be the same. Furthermore, the rate constants of both T1 reoxidation and T3 reduction were independent of protein or CO_2^- concentrations. These observations clearly showed that an intramolecular electron transfer process from T1 to T3 is induced following the initial reduction of T1[Cu(II)]. At pH 5.5 and $T = 298 \text{ K}$, the rate constants observed for the three unimolecular electron transfer steps were 201 ± 8 , 20 ± 4 and $2.3 \pm 0.2 \text{ s}^{-1}$, respectively [39]. No oxidation of T3[Cu(I)] could be observed during any of the monitored time frames.

The specific rates of the different intramolecular electron transfer steps were analyzed in the pH range from 5.5 to 7.0 [39]. Only a 20% decrease in the respective rate constants with increasing pH was observed. This is in line with the kinetic studies of AO activity by Nakamura et al. [41] who found that the O_2 reduction activity was practically constant between pH 5.5 and 7.0 yet decreased outside that range. The specific rates of the intramolecular electron transfer steps remained concentration independent over the pH range examined and their temperature dependence was determined at pH 5.5. The temperature dependence yielded activation enthalpies of 9.1 ± 1.1 and $6.8 \pm 1.0 \text{ kJ mol}^{-1}$ for the fast and slow intramolecular ET steps respectively, while the corresponding activation entropies were $-170 \pm 9 \text{ J K}^{-1} \text{ mol}^{-1}$ and $-215 \pm 16 \text{ J K}^{-1} \text{ mol}^{-1}$ [39]. The relatively small amplitudes of the intermediate electron transfer process precluded satisfactory analysis. Still, no marked temperature

dependence of the corresponding rate constant was noticed.

9. Implications of the intramolecular ET in ascorbate oxidase

The practical identity of the specific rates observed for both reoxidation of T1[Cu(I)] and the reduction of T3[Cu(II)] combined with their concentration independence and the similarity of their amplitudes, clearly support the assignment of the observed processes to intramolecular ET from T1 to T3. Two further labs have recently examined this system: Meyer et al. were the first to investigate the reduction of oxidized AO by the photochemically produced lumiflavin semiquinone and have observed a second-order reduction of the T1[Cu(II)] by the semiquinone ($2.7 \times 10^7 \text{ M}^{-1} \text{ s}^{-1}$, pH 7.0) followed by a partial reoxidation of the T1[Cu(I)] site (160 s^{-1} pH 7.0, 298 K) [38]. The employed experimental method did not enable monitoring spectral changes at 330 nm, where the presumed electron accepting T3[Cu(II)] site absorbs. Still, the process, monitored at 610 nm, was interpreted as an intramolecular T1[Cu(I)] to T3[Cu(II)] electron transfer [38]. No further absorption changes at slower time domains, analogous to our observation [39] were reported.

Pulse radiolytic studies of ascorbate oxidase have also been performed by Kyritsis et al. using both CO_2^- and several organic reducing radicals [40]. Two phases of T1 [Cu(I)] reoxidation were observed with rate constants, independent of the type or concentrations of radicals employed. While the agreement between the above results and our reported fast and slow rates is good, the reported 330 nm data (for reduction of the trinuclear centre) were inconclusive even when CO_2^- radicals were used [40]. This is in contrast to our results where clear concurrence was resolved between rates and amplitudes of the spectral changes at 610 nm (T1 Cu(I) reoxidation) and 330 nm (trinuclear Cu(II) reduction), cf. Fig. 5 [39]. Moreover, Kyritsis et al. assign the slow phase of internal ET to "further electron transfer from T1 to the trinuclear site following some (minor)

structural changes at the latter". There is a difficulty in accepting this proposal, namely it is unclear where these further electrons derive from under the employed conditions, when only a very limited degree of reduction is attained by each pulse. Also, the additional second phase is observed already in oxidized AO subjected to very low degree of reduction and not only in the partly reduced enzyme. Thus, we are currently inclined to assign the multiplicity of internal ET steps to the possible presence of AO species with distinct reactivity (cf. below).

Interestingly, using pulse-radiolytically produced reducing radicals (e.g. CO_2^- and O_2^-), we have previously observed an intramolecular ET from T1[Cu(I)] to T3[Cu(II)] in the related blue oxidase, *Rhus* laccase with a rate constant of $\sim 1.0 \text{ s}^{-1}$ (at pH 7.0 and 298 K). With this blue oxidase, however, no faster intramolecular ET events were seen [37].

The rate constant observed for the fast intramolecular ET phase is comparable to the reported limiting rate constants observed for AO reduction at high substrate concentration. Thus, a rate of 120 s^{-1} has been reported at pH 7.0 and 298 K with reductic acid as substrate [42], while using ascorbate at 283 K it was found to be $80\text{--}100 \text{ s}^{-1}$ [41]. These results are in line with the notion that the rate-limiting step in the enzymatic activity is the intramolecular T1[Cu(I)] to T3[Cu(II)] electron transfer.

In the three-dimensional structure of AO, the thiolate of Cys509 is resolved as one of the T1 copper ligands and the imidazole side chains of the two neighboring amino acids in this polypeptide sequence (His508 and His510) were shown to be ligands of the T3 copper ions [34,35]. This lead Messerschmidt, Huber and co-workers to propose that the shortest electron transfer pathway from T1[Cu(I)] to T3[Cu(II)] may be via residues Cys509 and either His508 or His510 (Fig. 6) [34]. Both pathways consist of nine covalent bonds yielding a total separating length of 1.34 nm (as compared with 0.90 nm for through space distance). An alternative pathway is provided by the carbonyl oxygen of Cys509 which is hydrogen bonded to the N δ of His508 has also been proposed. Using the pathway calculation method of Beratan and

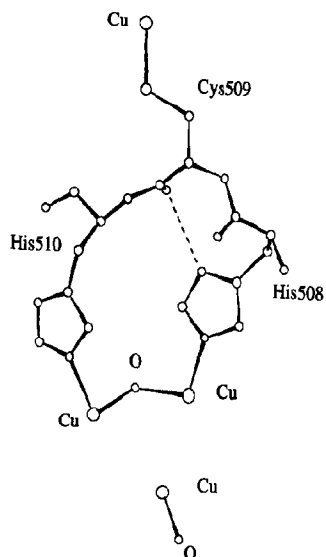


Fig. 6. Calculated ET pathways between the T1 Cu site (top) and the trinuclear centre (bottom) in AO. The hydrogen bond between O of Cys 509 and N δ of His508 is shown as a broken line. The calculation was based on the three-dimensional structure of this enzyme [34].

Onuchic [12,13], we have derived the relative electronic coupling between the electron donor and acceptor in these pathways. An electronic coupling value of 0.010 was calculated for ET through either of the first two covalent (through-covalent bond-only) pathways. For the alternative hydrogen-bond containing pathway, the coupling factor becomes 0.014, suggesting that, in fact, all three pathways are of practically equal probability.

The reorganization energy, λ can be derived from the activation parameters using the Marcus equation (Eq. (6)–(8)), cf. above. Using the through-bond distance (1.34 nm; Fig. 6) and the previously calculated value of β (6.7 nm $^{-1}$) for LRET in small proteins (cf. section 7) we find $\lambda = 153$ kJ mol $^{-1}$. This value is somewhat larger than those derived for the intramolecular ET in WT *Pseudomonas aeruginosa* azurin, where a $\lambda = 134$ kJ mol $^{-1}$ has been calculated, as discussed above. This is not unexpected considering the large structural changes at the trinuclear site which have been found to accompany reactions at this center [43,44].

Given the identity of the rate constants of T3 reduction and the T1 reoxidation, we may conclude that a single electron is transferred from the T1 site to T3 without T2 being reduced, and thus, T3[Cu(II)] can function as a one-electron acceptor. For a one-electron transfer from T1[Cu(I)] to T3[Cu(II)] we may calculate the equilibrium constant and find $K = 1.8$ (or $\Delta E'_{T3} - \Delta E'_{T1} = 15$ mV) at 298 K and pH 5.5. This value also explains how more than 50% of T1[Cu(I)] can be reoxidized in this intramolecular ET process. Also, the relatively slow intramolecular LRET rate constants are most probably due to the practical lack of driving force for the reaction at least under anaerobic conditions.

The observation of multiple phases in the intramolecular ET process [39] is noteworthy and is under further investigation. One possible rationale for this observation, has already been mentioned above, namely that it could be the result of the presence of distinct reactive forms, probably of the trinuclear center in the AO molecules. The recently determined 3D structures of several derivatives of AO [43,44], notably its fully reduced form, as well as the peroxo and azido complexes revealed the large extent of structural changes that are caused in the trinuclear center in the above AO derivatives. Thus, more limited structural variations could be caused in the fully oxidized AO by e.g. changes in the protonation state of the oxygen bridging ligand in this center (Fig. 6). Trying to resolve the nature and significance of this multiphasic internal ET process, we are currently investigating it as a function of an increasing degree of reduction of the AO molecules (attained by introducing sequential CO $_2^-$ pulses to the same, initially oxidized AO solution). The relative amplitudes of the distinct phases were markedly affected by the extent of AO reduction, while less consistent changes were observed in the rates (O. Farver, S. Wherland and I. Pecht, unpublished). Therefore, we do not assign these different phases to the varying reactivity of oxidase molecules reduced to different degrees. This is probably also excluded by the observation of these distinct phases via both chromophores, since the 330 nm band decays upon uptake of one electron and the multiple phases

are observed practically throughout a reductive titration. Earlier studies have however provided evidence for the existence of multiple blue oxidase species with different reactivities [45]. Thus, for example, it was suggested that reduction of T2 and T3[Cu(II)] of tree laccase is inhibited as long as an OH⁻ ion is bound to T2[Cu(II)]. The dissociation of the OH⁻ is apparently rather slow (a rate constant of 1 s⁻¹ for laccase [46] while for AO, a specific rate of 2 s⁻¹ [39] is observed for the slowest intramolecular electron transfer step). The high-resolution AO structure established the presence of water or hydroxide ion bound to the T2 and to the T3 copper site [34,35]. The hundredfold difference between the rate constants of the fastest and slowest intramolecular ET in AO cannot be due to different reorganization energies at the T3 sites having a coordinated water or OH⁻, since the activation enthalpies, (ΔH^*) of the fastest and slowest intramolecular e.t. phases are, within the experimental error, the same. The difference in rate constants is an entropic effect and may be attributed to AO molecules with different conformations of the trinuclear centre.

Acknowledgement

We acknowledge the support by the German-Israeli Foundation of the research described in this report. The authors wish to thank Dr. Lars K. Skov for producing the figures of the protein structures.

References

- [1] R.A. Marcus and N. Sutin, *Biophys. Biochim. Acta* 811 (1985) 265.
- [2] M.J. Clarke et al., eds., *Long Range Electron Transfer in Biology, Struct. Bonding* 75 (1991) 1.
- [3] A. Broo and S. Larsson, *Chem. Phys.* 148 (1990) 103.
- [4] J. Jortner and M. Bixon, *Mol. Cryst. Liquid. Cryst.* 234 (1993) 29.
- [5] O. Farver and I. Pecht, in: *Copper proteins and copper enzymes*, Vol. 1, (ed. R. Lontie) (CRC, Boca Raton, 1984) p. 183.
- [6] W.E.B. Shepard, B.F. Anderson, D.A. Lewandoski, G.E. Norris and E.N. Baker, *J. Am. Chem. Soc.* 112 (1990) 7817.
- [7] M. Plato, M.E. Michel-Beyerle, M. Bixon and J. Jortner, *FEBS Letters* 249 (1989) 70.
- [8] S. He, S. Modi, D.S. Bendall and J.C. Gray, *EMBO J.* 10 (1991) 4011.
- [9] H. Pelletier and J. Kraut, *Science* 258 (1992) 1748.
- [10] A. Kuki and P.G. Wolynes, *Science* 236 (1987) 1647.
- [11] S. Franzen and S.G. Boxer, *J. Phys. Chem.* 97, (1993) 6304.
- [12] D.N. Beratan, J.N. Betts and J.N. Onuchic, *Science* 252 (1991) 1285.
- [13] J.N. Onuchic, D.N. Beratan, J.R. Winkler and H.B. Gray, *Ann. Rev. Biophys. Biomol. Struct.* 21 (1992) 349.
- [14] E.J. Hart and M. Anbar, *The hydrated electron* (Wiley, New York 1970).
- [15] M.H. Klapper and M. Faraggi, *Quart. Rev. Biophys.* 12 (1979) 465.
- [16] E.T. Adman, *Advan. Prot. Chem.* 42 (1991) 145.
- [17] E.T. Adman, *Topics in Molecular and Structural Biology. Metalloproteins* ed. P.M. Harrison (Verlag Chemie, Berlin, 1985).
- [18] E.N. Baker, *J. Mol. Biol.* 203 (1988) 1071.
- [19] H. Nar, A. Messerschmidt, R. Huber, M. v.d. Kamp and G.W. Canters, *J. Mol. Biol.* 218 (1991) 427.
- [20] H. Nar, A. Messerschmidt, R. Huber, M. v.d. Kamp and G.W. Canters, *J. Mol. Biol.* 221 (1991) 765.
- [21] O. Farver and I. Pecht, *Proc. Natl. Acad. Sci. USA* 86 (1989) 6968.
- [22] O. Farver and I. Pecht, *J. Am. Chem. Soc.* 114 (1992) 5764.
- [23] O. Farver, L.K. Skov, M. v.d. Kamp, G.W. Canters and I. Pecht, *Eur. J. Biochem.* 210 (1992) 399.
- [24] O. Farver, L.K. Skov, T. Pascher, B.G. Karlsson, M. Nordling, L.G. Lundberg, T. Vännegård and I. Pecht, *Biochemistry* 32 (1993) 7317.
- [25] T. Pascher, B.G. Karlsson, M. Nordling, B.G. Malmström and T. Vännegård, *Eur. J. Biochem.* 212 (1993) 289.
- [26] H.B. Gray and J.R. Winkler, *Pure Appl. Chem.* 64 (1992) 1257.
- [27] A. Broo and S. Larsson, *J. Phys. Chem.* 95 (1991) 4925.
- [28] C.C. Moser, J.M. Keske, K. Warncke, R.S. Farid and P.L. Dutton, *Nature* 355 (1992) 796.
- [29] R.S. Farid, C.C. Moser and P.L. Dutton, *Curr. Biol.* 3 (1993) 225.
- [30] D.N. Beratan, J.N. Onuchic, J.R. Winkler and H.B. Gray, *Science* 258 (1992) 1740.
- [31] D.S. Wuttke, M.J. Bjerrum, I.-J. Chang, J.R. Winkler and H.B. Gray, *Biochim. Biophys. Acta* 1101 (1992) 168.
- [32] A. Messerschmidt, *Bioinorganic chemistry of copper*, eds. K.D. Karlin and Z. Tyeklár (Chapman and Hall, New York, 1993).
- [33] A. Marchesini and P.M.H. Kroneck, *Eur. J. Biochem.* 101 (1979) 65.
- [34] A. Messerschmidt, A. Rossi, R. Ladenstein, R. Huber, M. Bolognesi, G. Gatti, A. Marchesini, R. Petrucelli and A. Finazzi-Agró, *J. Mol. Biol.* 206 (1989) 513.

- [35] A. Messerschmidt and R. Huber, *Eur. J. Biochem.* 187 (1990) 341.
- [36] P.M.H. Kroneck, F.A. Armstrong, H. Merkle and A. Marchesini, *Advan. Chem. Ser.* 220 (1982) 223.
- [37] O. Farver and I. Pecht, *Mol. Cryst. Liquid. Cryst.* 194 (1991) 215.
- [38] T.E. Meyer, A. Marchesini, M.A. Cusanovitch and G. Tollin, *Biochemistry* 30 (1991) 4619.
- [39] O. Farver and I. Pecht, *Proc. Natl. Acad. USA* 89 (1992) 8287.
- [40] P. Kyritsis, A. Messerschmidt, R. Huber, G.A. Salmon and A.G. Sykes, *J. Chem. Soc. Dalton Trans.* (1993) 731.
- [41] T. Nakamura and Y. Ogura, *J. Biochem.* 64 (1968) 189.
- [42] A. Baici, P.L. Luisi, S. Palmieri and A. Marchesini, *J. Mol. Catal.* 6 (1979) 135.
- [43] A. Messerschmidt, R. Ladenstein, R. Huber, M. Bolognesi, L. Avigliano, R. Petruzzeli, A. Rossi and A. Finnazi-Agró, *J. Mol. Biol.* 224 (1992) 179.
- [44] A. Messerschmidt, H. Luecke and R. Huber, *J. Mol. Biol.* 230 (1993) 997.
- [45] M. Goldberg, O. Farver and I. Pecht, *J. Biol. Chem.* 255 (1980) 7353.
- [46] B. Reinhammar, *The coordination chemistry of metalloenzymes*, eds. I. Bertini, R.S. Drago and C. Luchinat (Reidel, Dordrecht, 1983) p. 177.